

1 m12b: Evolution of most-aligned (and unaligned) samples at infall

Orbital dispersion reaches a minimum for each most-aligned subsample near LMC analog pericenter. Orbital dispersion also trends down for the ‘unaligned’ samples from infall to pericenter. At right, the angle between the LMC analog’s orbital pole and the average for each most-aligned subsample stays relatively constant, but the angle between the unaligned samples and the LMC analog trends downward over time, even after pericenter and dips noticeably near the second pericenter of the LMC analog.

NOTE: the LMC analog merges into the MW host around $t=11$ Gyr (see plot in section 5), after this point the orb dispersion is calculated wrt each sample’s own average.

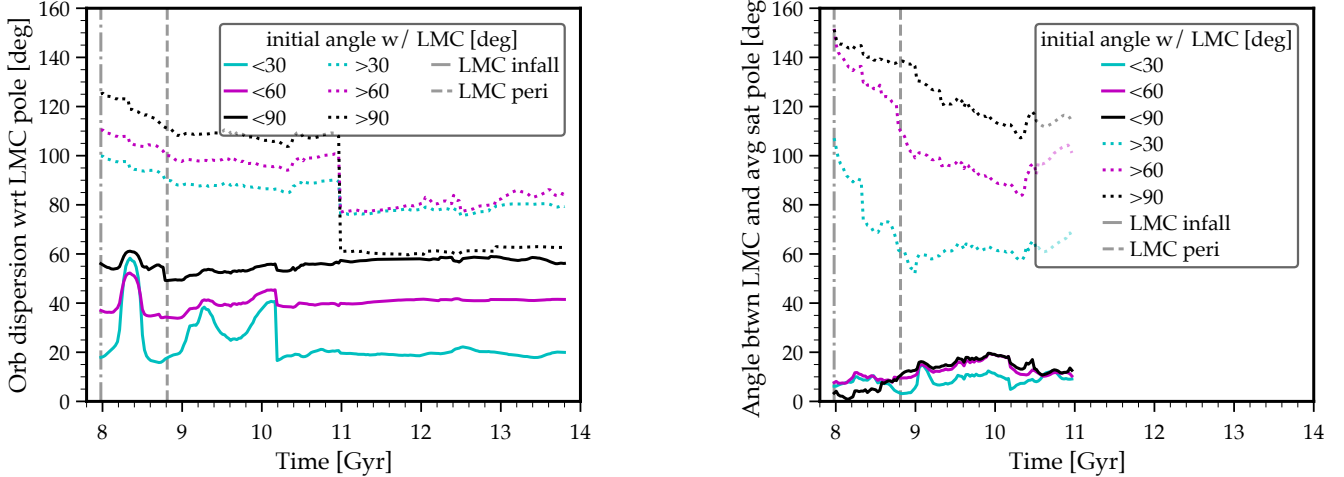


Figure 1: *Left:* Orbital pole dispersion for subsamples of satellites most-aligned with the LMC analog’s orbital pole at infall, tracked forward in time. Dotted lines are the opposite of each most-aligned selection, to give an idea of how the initially unaligned sample is affected by the LMC analog. *Right:* Angle between each sample’s average orbital pole and the LMC analog’s orbital pole over time. Lines stop when LMC analog has merged.

2 Separation of host halo and disc centers over time

Each host trends toward smaller distances between halo and disc center as time goes on, with a noticeable downward trend between LMC analog infall and pericenter.

NOTE: something strange happening with this quantity right near $z = 0$.

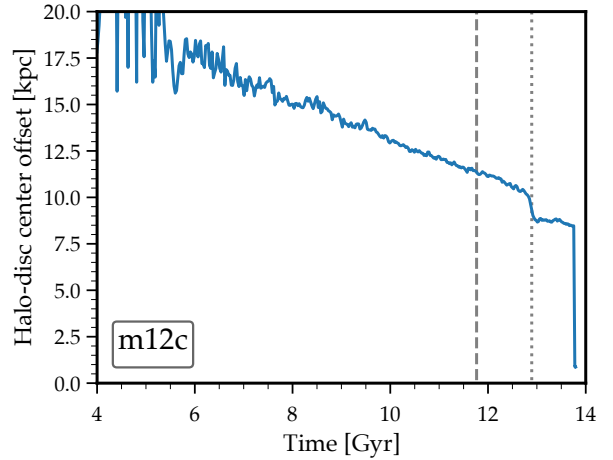
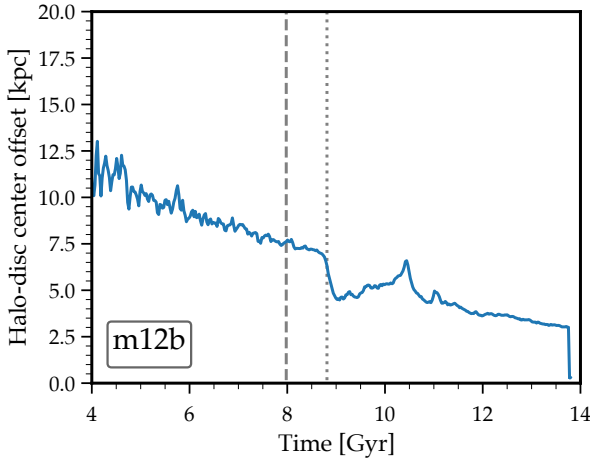


Figure 2:

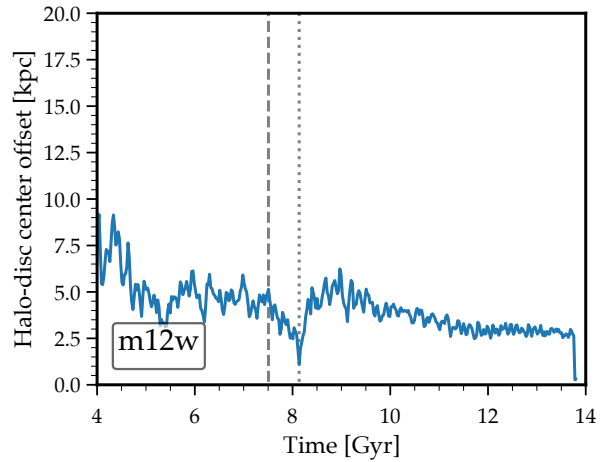
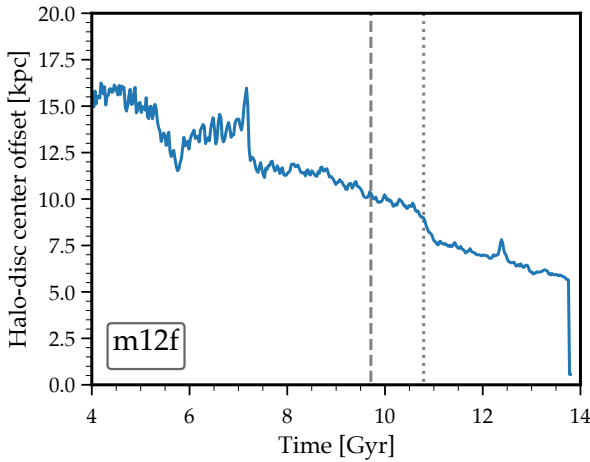


Figure 3:

3 First orbital pole measurements for all 4 LMC analogs

3.1 Peak subhalo mass selection

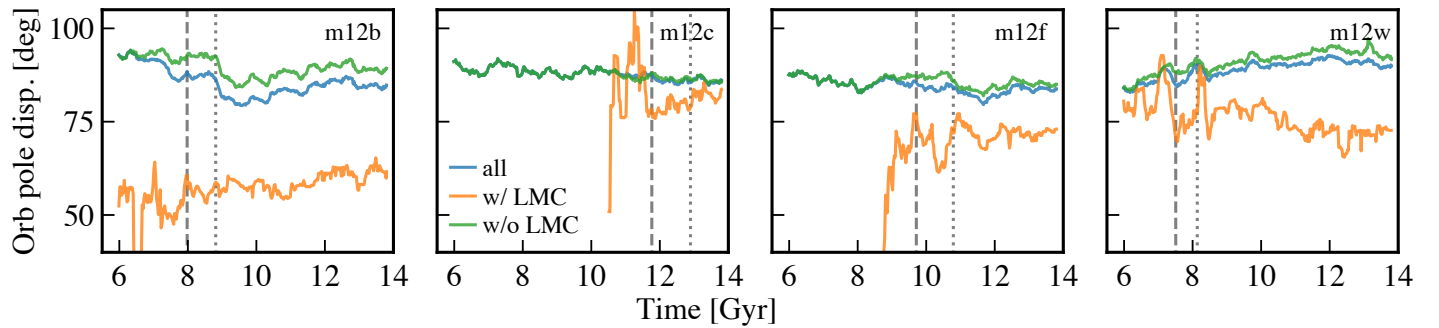


Figure 4: Orbital dispersion for all subhalos with $M_{peak} > 10^8 M_\odot$.

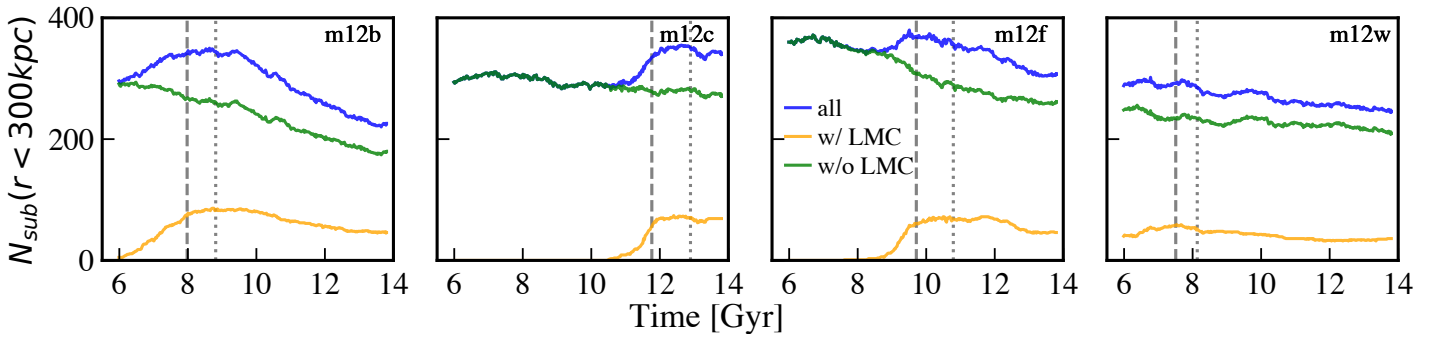


Figure 5: Number of subhalos with $M_{peak} > 10^8 M_\odot$.

3.2 Minimum number of star particles (6) selection

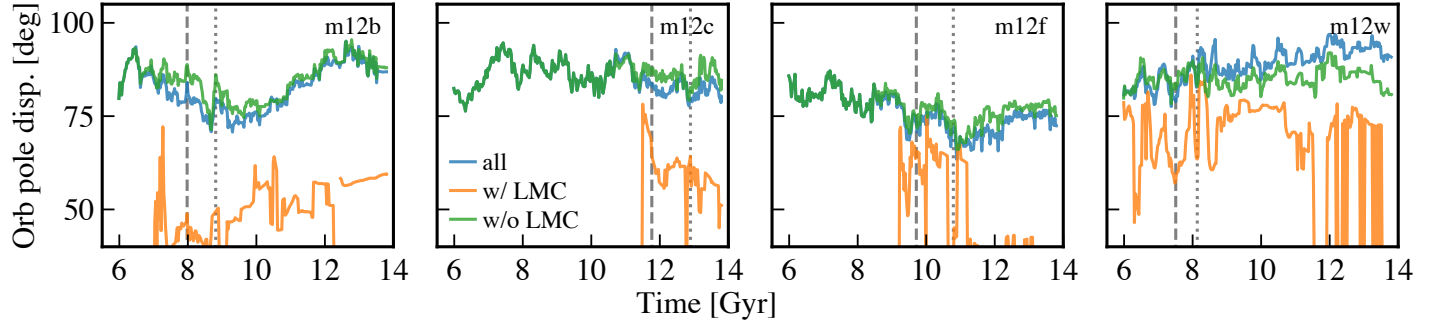


Figure 6: Orbital dispersion for all luminous satellites with at least 6 star particles.

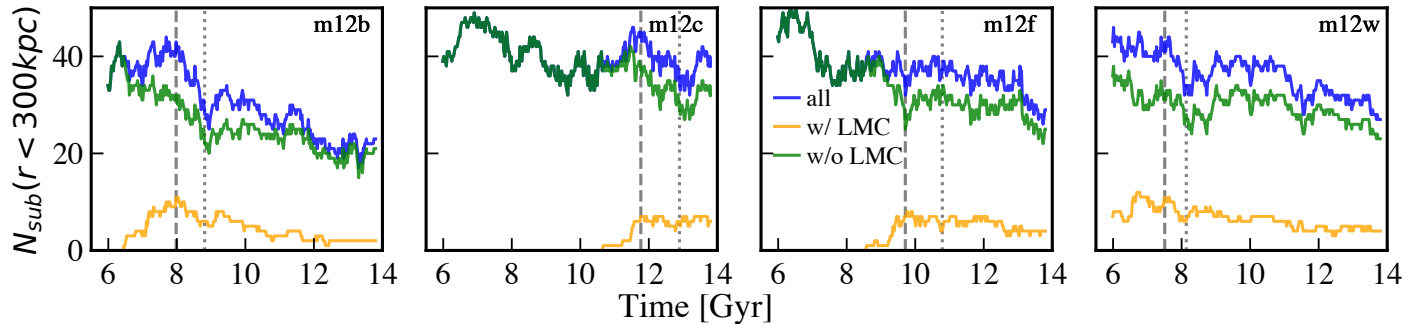


Figure 7: Number of subhalos with $N_{star} \geq 6$.

4 Motion of the host disc normalized to an earlier time

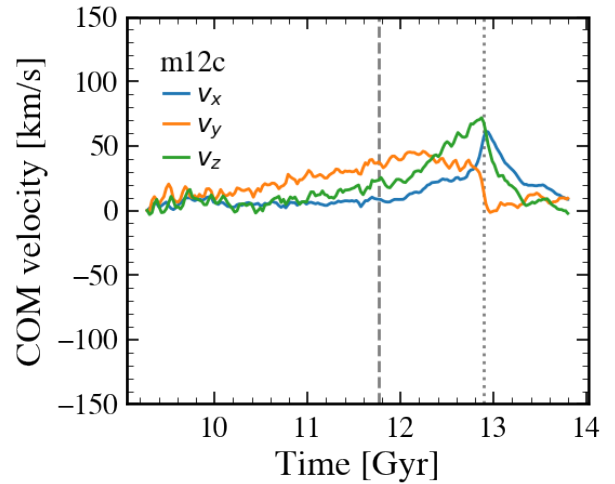
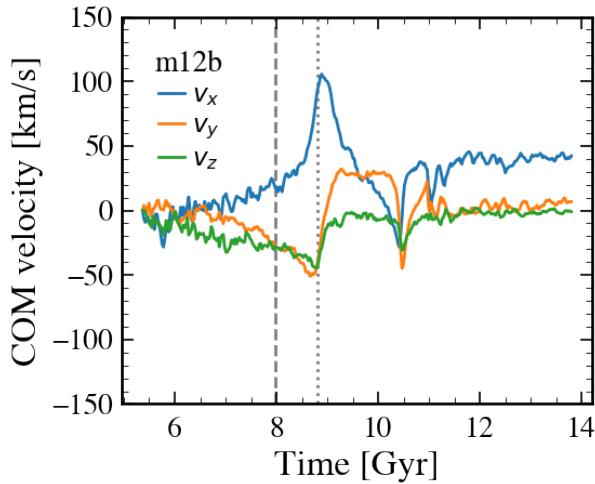


Figure 8: COM host disc motion relative to ~ 2.5 Gyr before LMC analogue infall. Arbitrary axes.

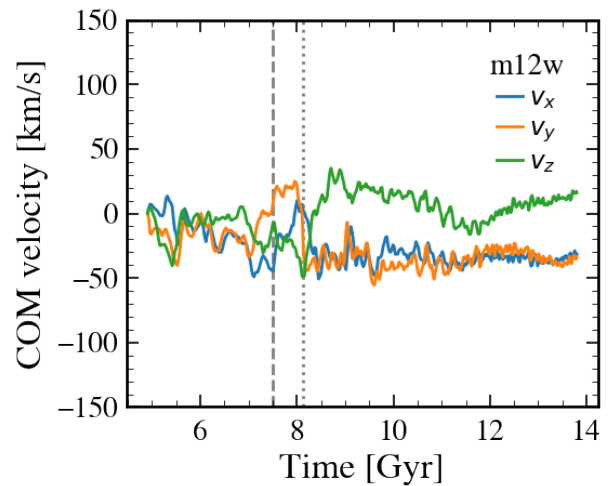
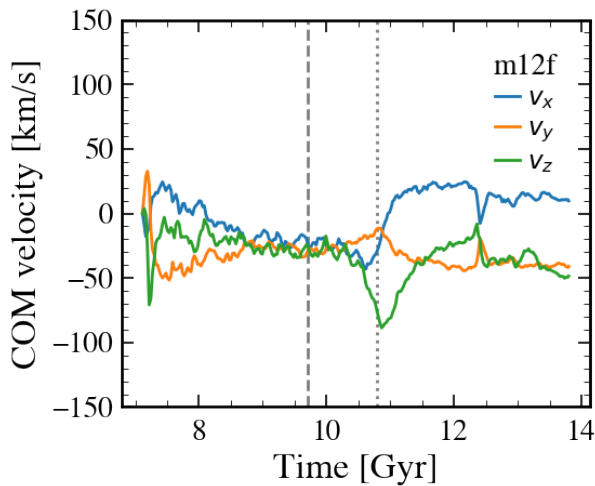


Figure 9: COM host disc motion relative to ~ 2.5 Gyr before LMC analogue infall. Arbitrary axes.

5 LMC properties from Sierra's work

Table 1: Properties of the LMC satellite analogues at their first pericentric passage about their MW/M31-mass host in our FIRE-2 simulations. We select satellites with $M_{\text{sub,peak}} > 4 \times 10^{10} M_{\odot}$ and $M_* > 10^9 M_{\odot}$ that have their first pericenter after 7.5 Gyr ($z < 0.7$) and within 50 kpc of their host.

Host	$M_{\text{sub,bound}} [10^{10} M_{\odot}]$	$M_{\text{sub,peak}} [10^{11} M_{\odot}]$	$M_* [10^9 M_{\odot}]$	$t_{\text{peri}} [\text{Gyr}]$	z_{peri}	$d_{\text{peri}} [\text{kpc}]$
m12b	12.0	2.1	7.1	8.8	0.49	38
m12c	5.1	1.6	1.2	12.9	0.07	18
m12f	6.0	1.5	2.6	10.8	0.26	36
m12w	4.9	0.8	1.3	8.0	0.59	8

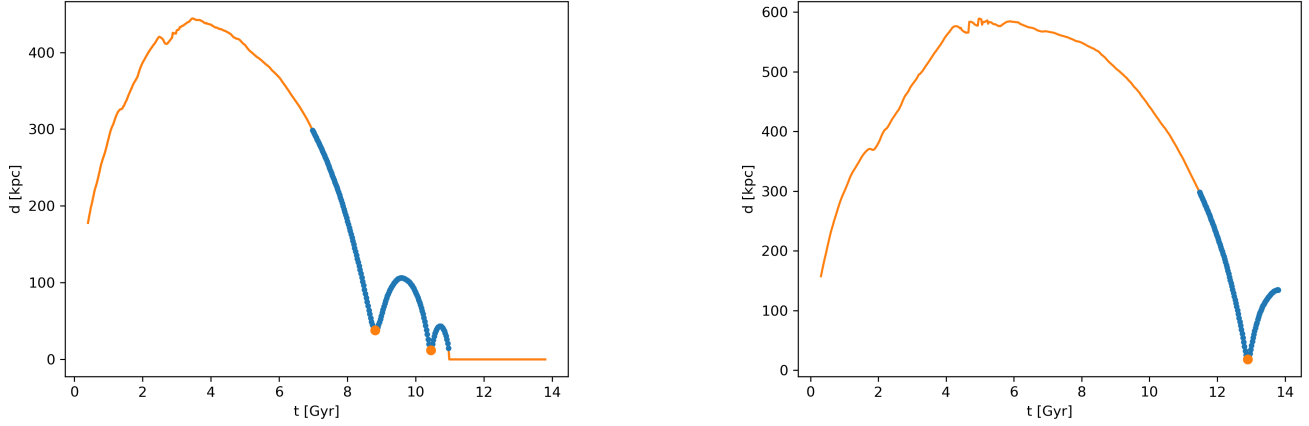


Figure 10: LMC orbits for m12b (left) and m12c (right).

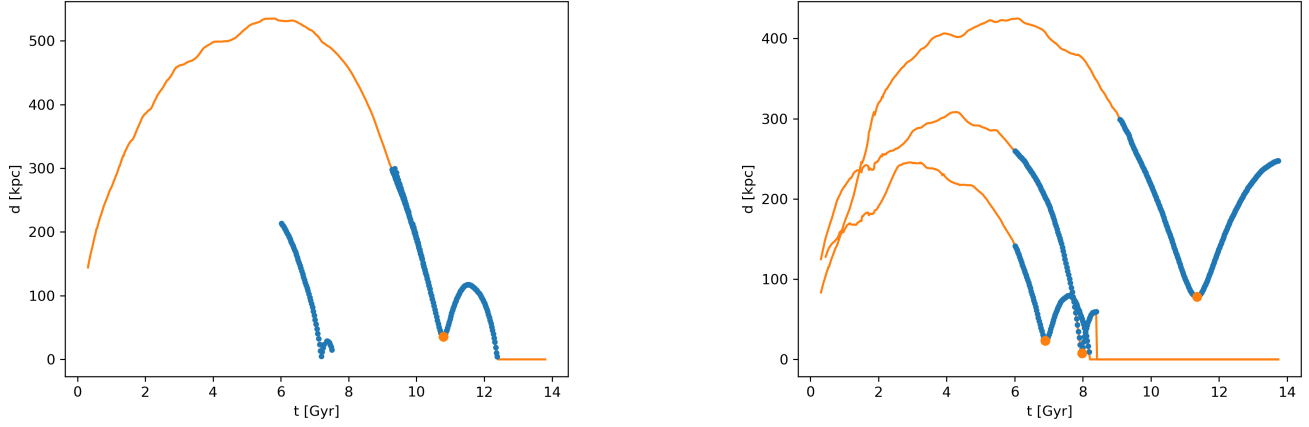


Figure 11: LMC orbits for m12f (left) and m12w (right).